

## Appendix G-1: Ozone Sensitivity to NO<sub>x</sub> Emissions

## Ozone Sensitivity to NO<sub>x</sub> Emissions

March 16, 2007

J. C. Hains  
Department of Chemistry  
University of Maryland  
College Park, MD

**1. Why is this analysis important?**

In order to improve air quality model performance, it is necessary to understand how NO<sub>x</sub> emissions affect ozone, which is the focus of this analysis.

**2. What questions are answered by this analysis?**

How is measured ozone in the Mid-Atlantic region affected by NO<sub>x</sub> emissions?  
Do ozone concentrations between 100 and 2500 m altitude vary with regional NO<sub>x</sub> emissions?

**3. What are the key take-away messages of this analysis?**

Although a nonlinear relationship is predicted from photochemical analyses, ozone concentration varied linearly with integrated upwind NO<sub>x</sub> emissions.  
A given percent reduction of NO<sub>x</sub> should result in an equal percent reduction of ozone.

**4. What conclusions are reached in this analysis with respect to Maryland's attainment demonstration?**

CMAQ shows that although model simulated NO<sub>x</sub> reductions result in ozone reductions, the percentage reductions in ozone were smaller than the percentage reductions in NO<sub>x</sub>. This analysis suggests that CMAQ may underestimate the effect of NO<sub>x</sub> reductions on ozone levels.

## Abstract

Upwind power plant emission sources of NO<sub>x</sub> and SO<sub>2</sub> from West Virginia, Ohio, and Pennsylvania along the Ohio River Valley play a crucial role in the amount of ozone and aerosol measured in the lower troposphere in the Mid-Atlantic region. Greater NO<sub>x</sub> emissions along back trajectories were positively correlated with greater ozone mixing ratios measured by 232 aircraft vertical profiles performed in the Mid-Atlantic and Northeast U.S. between 1997 and 2003. Ozone column contents during the flights are strongly influenced by point source emissions with a slope of 61.6 ppbv ozone / (g NO<sub>x</sub> m<sup>-2</sup> day<sup>-1</sup>), an intercept of 1.3 ppbv, and a correlation ( $r^2$ ) of 0.997 (e.g. Hains *et al.*, 2007).

## Introduction

In this analysis a hierarchical clustering method was used to separate distinct chemical and meteorological events from 232 lower tropospheric aircraft vertical profiles measuring ozone in the Mid-Atlantic and Northeast U.S. between 1997 and 2003. NOAA HYSPLIT 48-hour back-trajectories ending at 1 km (above ground level), using EDAS 80 km meteorology and modeled vertical velocity, were run for each profile to determine the most influential NO<sub>x</sub> sources. When examining individual episodes, 24-hour back-trajectories are better than 48-hour back-trajectories because there are fewer fluctuations in the meteorology. However, when examining more than one episode, 48-hour back-trajectories are more suitable. This is especially true for large sets of ozone episodes, because ozone has a lifetime longer than a single day. For this reason 48-hour back-trajectories were used in this analysis. The 2-day integrated NO<sub>x</sub> emissions encountered by each trajectory were calculated using the EPA Clean Air Market Division point source emissions database. A regression was made between the median integrated NO<sub>x</sub> emissions and the median ozone column contents for each cluster to determine the relationship between NO<sub>x</sub> emissions and ozone. Only point source integrated NO<sub>x</sub> emissions were examined. There is a positive correlation between point and area source emissions, and the relationship between point source NO<sub>x</sub> emissions and ozone should be extended to include area source NO<sub>x</sub> emissions as well.

## Methods

A statistical cluster analysis generally involves determining the differences between the objects being analyzed, and grouping those objects with the smallest differences. Taubman *et al.*, (2006) examined statistics for University of Maryland research aircraft profiles of ozone and showed median profiles and the statistical spread around those profiles. Ozone showed distinctive profiles (Taubman *et al.*, 2006); for example, ozone was most concentrated above 500 m in the morning and was more uniform from the surface to 2000 m in the afternoon (the largest values in the profiles were found near the 1100 m level). The differences between each pair of profiles were calculated in a manner similar to that described in Hains *et al.*, 2007.

The raw data were averaged into altitude layers of 100 m, and then the averages were grouped into bins shown in Table 1. The slope and correlation of the points in each pair of profiles under comparison were considered as well as the total difference in mixing ratio between the two profiles within each altitude bin. The following equation was used to calculate the differences among the aircraft profiles:

$$D_{ij} = \sum_{k=1}^{k=4} \left\{ \underbrace{\left( \sum_{a=n}^{a=m} abs(c_{ia} - c_{ja}) \right)^2}_{Part\_1} * \underbrace{\left( 1 + [1 - R] + [1 - \exp(-(s - 1)^2)] \right)}_{Part\_2} \right\} \text{ Equation 1}$$

Here,  $k$  denotes four different altitude bins for the trace gas profiles, and  $a$  denotes the 100 m layers ( $n$  through  $m$  within each altitude bin (Table 1). The species value is represented by  $c$  for the  $i^{\text{th}}$  and  $j^{\text{th}}$  profile. In each altitude bin,  $k$ , there are at least four 100 m layers of ozone data. A regression between the ozone mixing ratios for each pair of profiles at the four layers in each of the bins was used to obtain the slope,  $s$ , and the correlation coefficient,  $R$ . The first part of Equation 1 determines the square of the sum of the differences between values at each altitude level,  $k$ . The second part of the equation multiplies the difference by one plus differences associated with the correlation and slope. When the correlation is small or negative, the profiles are very different and the  $1 - R$  portion increases, which increases the total difference  $D_{ij}$ . The exponent of the slope portion is used to account for the slope between the pairs of profiles. A slope near unity suggests that the profiles are similar and thus should add little to the total difference. The exponent of the slope was used to guarantee that slopes much different from unity will make the exponential term small and thus increase the total difference. Once the difference between each pair of profiles was calculated, the profiles with the smallest differences were clustered together using a standard hierarchical agglomerative clustering algorithm in Matlab.

Table 1. Altitude bins used in Equation 1.

k level	Altitude bins for ozone
1	151-650 m
2	651-1150 m
3	1151-1650 m
4	1651-2450 m

## Results and Discussion

Figure 1 shows the median profiles for each of the six ozone clusters calculated in the above manner. Figure 2 shows back trajectory density plots for five of the clusters. These were generated from back trajectories that terminated at the location and time the profile was made. Flights were made from North Carolina to Maine between 1997 and 2003, and these are shown in Figure 3. Cluster 6 has very large values of ozone measured above 2000 m. There are only two profiles in this cluster, and they were made on 8 and 9 July 2002 when smoke from Canadian forest fires impacted the Mid-Atlantic region (Colarco et al., 2004; Taubman et al., 2004). The transported ozone can be seen in the peak (up to 150 ppbv) above 2 km.

Profiles from clusters 3, 4 and 5 had large ozone values (Figure 1) and the back trajectory density plots (Figure 2) show passage over the Northern Ohio River Valley, where there is a high concentration of  $\text{NO}_x$  sources. Taubman et al. (2006) found a similar relationship between back trajectories concentrated over the Northern Ohio River Valley and large values of ozone and suggested that the high concentration of power plants in this region contribute to ozone in the Mid-Atlantic region. The back trajectory density plots for clusters 3, 4 and 5 also show large densities around the I-95 corridor, which is suggestive of weak winds that lead to higher ozone values. Cluster 2 has the

smallest ozone values and back trajectories that cross over the Atlantic Ocean, which may explain the small ozone values associated with this cluster. Cluster 1 has the second smallest ozone values (cluster 1 column content is 19% less than clusters 3), however, the back trajectories associated with cluster 1 are similar to those of cluster 3. To address this discrepancy, the integrated  $\text{NO}_x$  point source emissions along the back trajectories were examined.

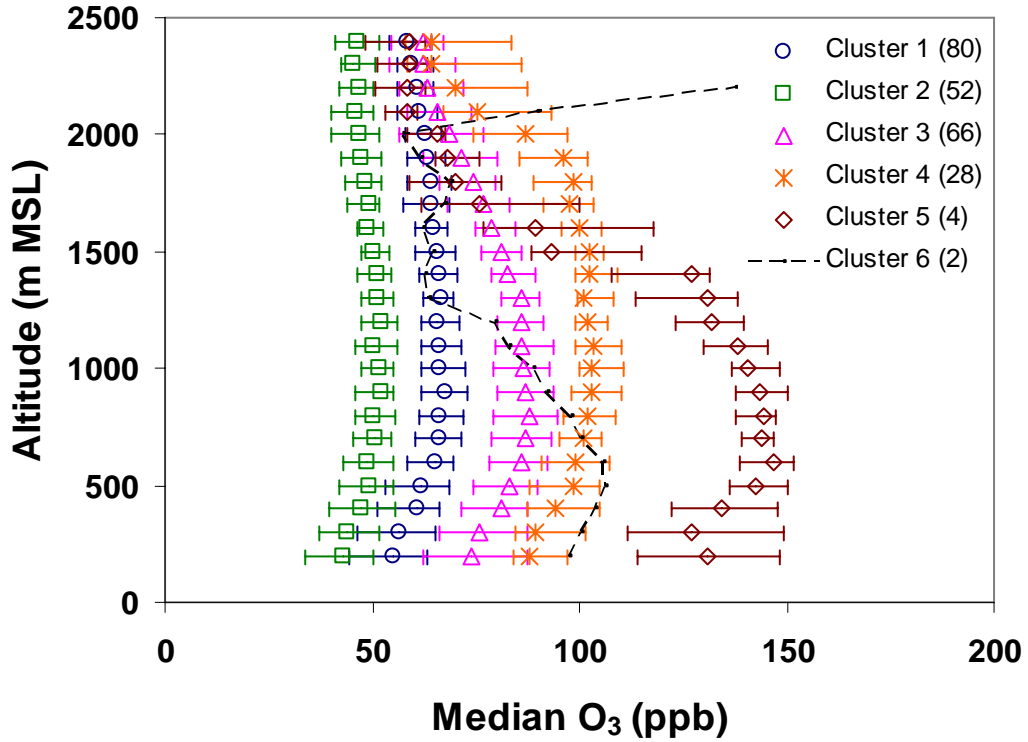


Figure 1. Median ozone profiles for each of the six clusters. Error bars represent the 25<sup>th</sup> and 75<sup>th</sup> percentiles. The number of profiles in each cluster is shown in parentheses in the key. Cluster 1 and 2 show the smallest ozone values while clusters 3, 4, and 5 show the largest. Cluster 6 profiles were made when the Canadian forest fire impacted the region and the peak above 2 km shows its impact.

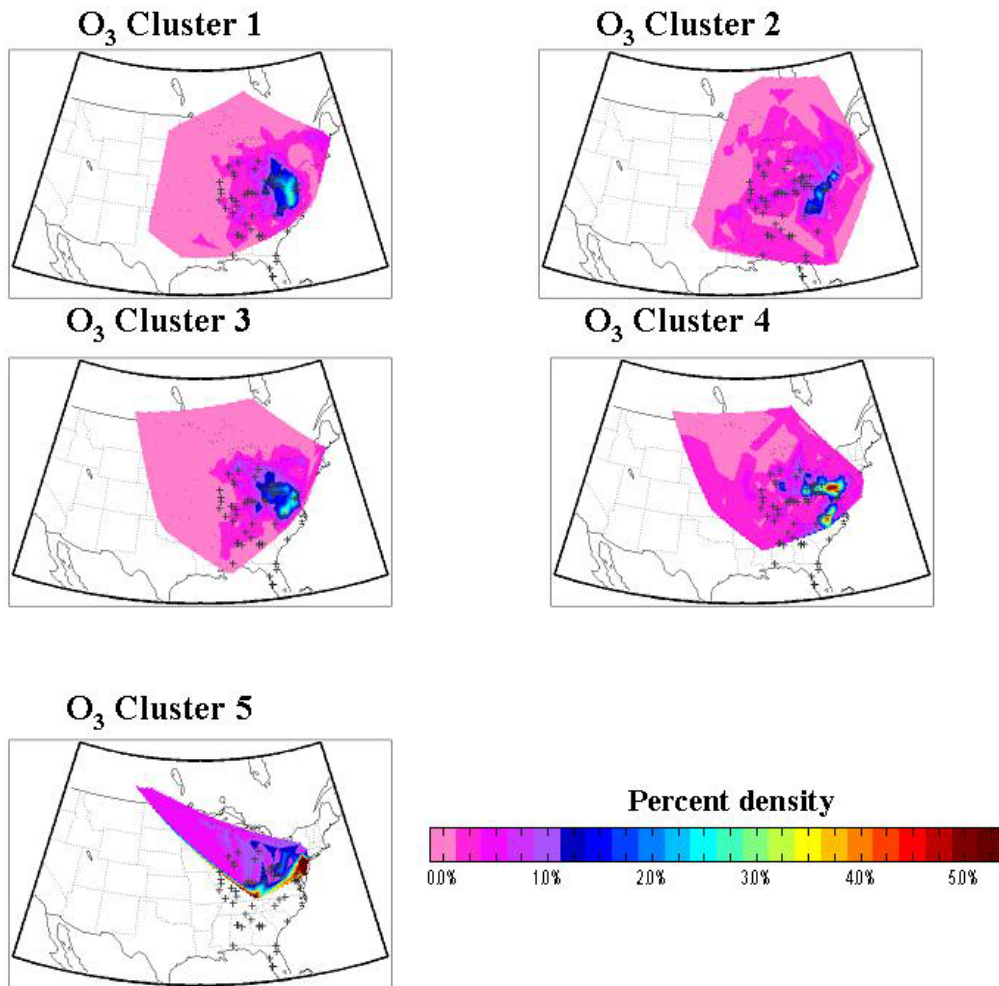


Figure 2. Back trajectory density plots for ozone clusters 1-5. The largest 0.3% NO<sub>x</sub> sources are shown with a + symbol. Clusters 3, 4, and 5, associated with larger ozone values, show larger densities near point sources as well as along the I-95 corridor. Clusters 1 and 2, with low ozone mixing ratios, are associated with more variable winds.

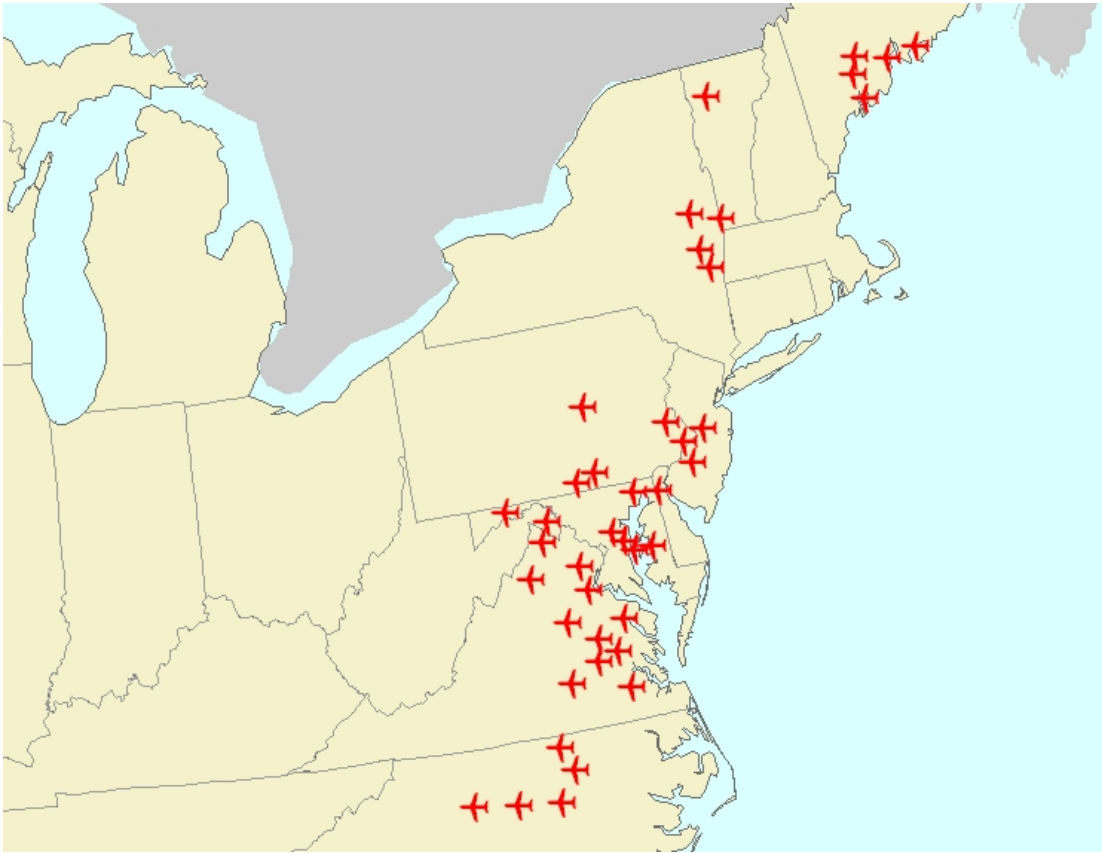


Figure 3. Locations of University of Maryland research aircraft flight spirals made in the eastern United States between 1997 and 2003

To understand the influence of emissions upwind of the spiral locations, the integrated  $\text{NO}_x$  emissions along each back trajectory were calculated. Emissions from the daily EPA Clean Air Market unit level emissions database (<http://cfpub.epa.gov/gdm/index.cfm?fuseaction=emissions.wizard>) were used in this analysis. A circle was drawn, centered at each back trajectory position for each hour of the two day back trajectory (Figure 4). The radius of the circle was 80 km to account for uncertainties associated with the back trajectory position and the influence of eddy diffusion and mixing processes. The emissions within each circle were summed. The sum of the emissions for each circle was divided by the area of the circle. The emissions from the day on which the back trajectory crossed a circle were used for the date of each back trajectory position. The summed emissions will be referred to as integrated emissions. Statistics (median, 5<sup>th</sup>, 25<sup>th</sup>, 75<sup>th</sup> and 95<sup>th</sup> percentiles) for the integrated  $\text{NO}_x$  emissions are shown in Figure 5.

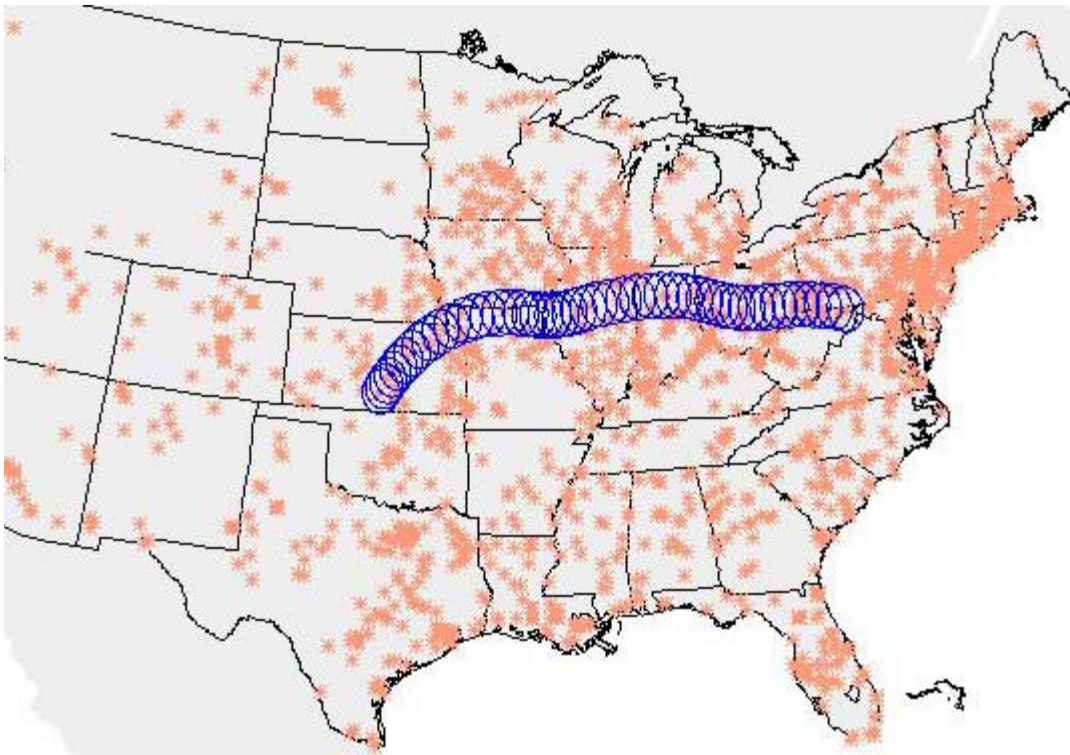


Figure 4. Circles drawn around an example back trajectory. The emissions contained in each circle were summed and divided by the area of the circle. Then emissions from each circle were summed. Each asterisk represents a point source location (all point sources in the domain are shown).



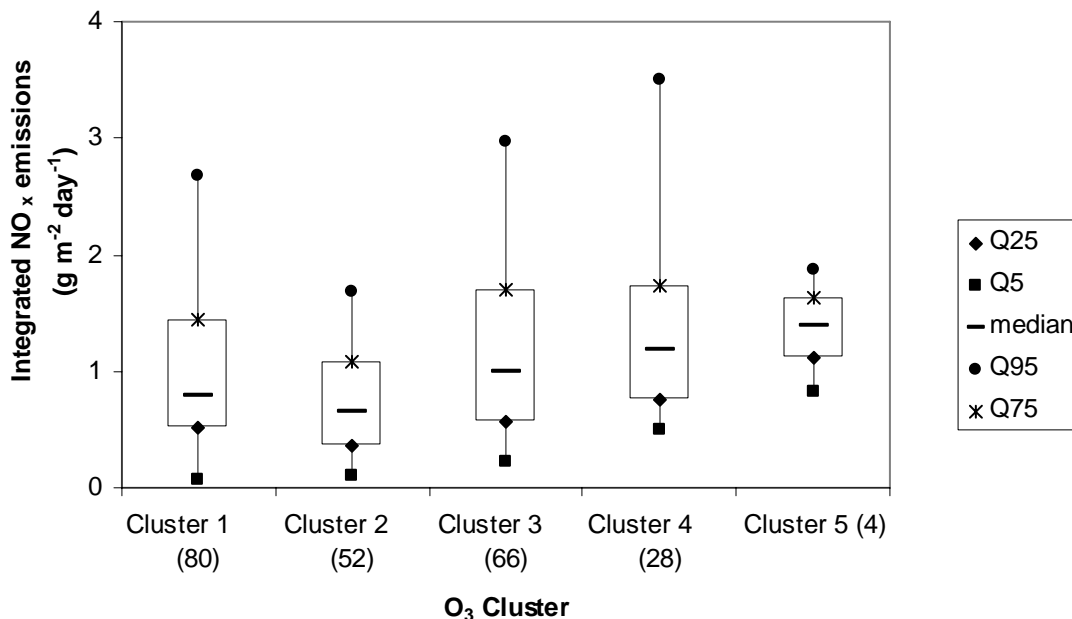


Figure 5. Statistics for NO<sub>x</sub> emissions encountered by back trajectories for each ozone cluster. The NO<sub>x</sub> emissions are sums of all emissions (g day<sup>-1</sup>) encountered by a back trajectory divided by the area of the circle drawn around the back trajectory point (m<sup>2</sup>). Clusters 1 and 2, with the smallest ozone values are also associated with the smallest NO<sub>x</sub> emissions. Clusters 3, 4 and 5, with the largest ozone values, are associated with the largest NO<sub>x</sub> emissions.

Ozone column contents were calculated by integrating the profiles from 100 m to 2500 m; these column contents were converted to average column contents in ppbv, assuming standard temperature and pressure (273.15 K and 1 atm). Note that this is not a measurement of ozone at the surface but what the ozone mixing ratio would be in a profile with a constant mixing ratio. Clusters 3, 4 and 5 have the largest ozone values and the largest NO<sub>x</sub> emissions, while clusters 1 and 2 have the smallest ozone values and the smallest NO<sub>x</sub> emissions. The median ozone column content was regressed against the integrated NO<sub>x</sub> emissions (Figure 6). The correlation coefficient,  $r^2$ , of 0.997 is very high. The slope is 61.6 ppbv ozone / (g NO<sub>x</sub> m<sup>-2</sup> day<sup>-1</sup>) with an intercept of 1.3 ppbv ozone. The slope of the line in Figure 6 does not provide a quantitative evaluation of the relationship of ozone mixing ratio with NO<sub>x</sub> emissions, but it does indicate that ozone is related to point source NO<sub>x</sub> emissions and a reduction in NO<sub>x</sub> corresponds to roughly the same reduction in ozone. Part of the reason for positive correlation between ozone and point source NO<sub>x</sub> emissions is that point sources are correlated with area sources of NO<sub>x</sub>. Figure 7 shows a positive relationship between area and point source emissions of NO<sub>x</sub> from eight states in the Mid-Atlantic region.

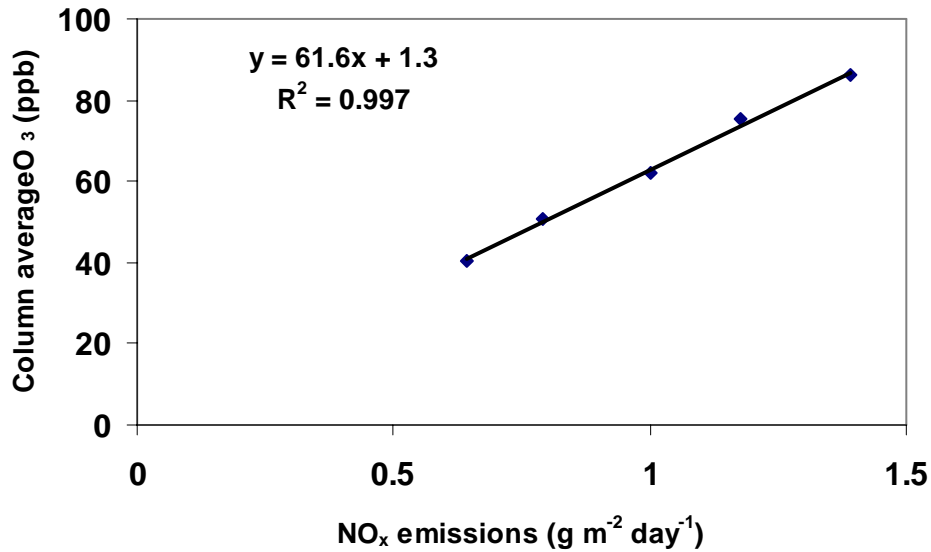


Figure 6. Median ozone column average and median integrated NO<sub>x</sub> emissions (from point sources) for ozone clusters 1-5. The ozone is positively correlated with integrated NO<sub>x</sub> emissions.

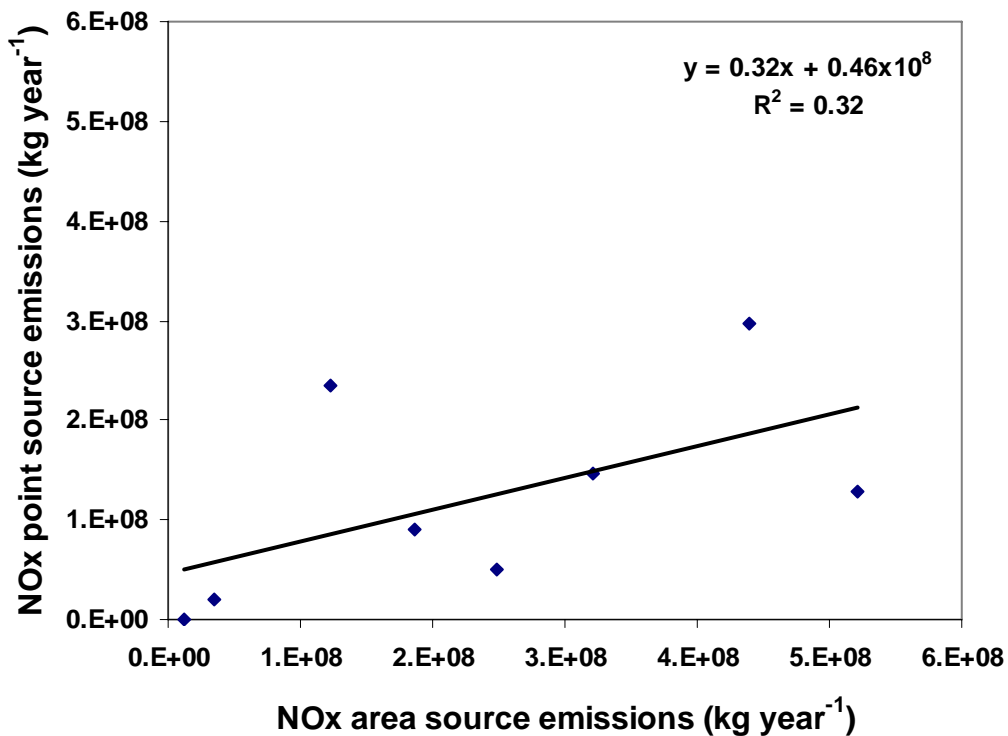


Figure 7. A regression between the sum of NO<sub>x</sub> area sources and NO<sub>x</sub> point sources for eight locations in the Mid-Atlantic region (District of Columbia, Delaware, Maryland, New Jersey, New York, Pennsylvania, Virginia, and West Virginia). There is a positive correlation between point and area sources of NO<sub>x</sub>.

Profiles were also grouped by time of day, where morning profiles are defined as those made before 12:00 noon EST and afternoon profiles are defined as after 12:00 noon EST. Sixty-one and sixty-eight percent of the profiles in clusters 3 and 4 were measured in the afternoon, whereas only 38% of the profiles in clusters 1 and 2 were measured in the afternoon. Greater ozone values in clusters 3 and 4 may be partly explained by the increased number of afternoon profiles, which were generally made downwind of urban centers, and had a longer time period for ozone production.

## **Conclusions**

A cluster analysis of ozone profiles was performed to determine meteorological and point source influences on the profiles. Profiles with elevated levels of ozone are positively correlated with NO<sub>x</sub> point source emissions encountered by a 48-hour back-trajectory. The linear regression of ozone column content and integrated NO<sub>x</sub> emissions (from a 48-hour back-trajectory) gives a slope of 61.6 ppbv ozone / (g NO<sub>x</sub> m<sup>-2</sup> day<sup>-1</sup>), intercept of 1.3 ppbv and a correlation coefficient, r<sup>2</sup>, of 0.997. Point source emissions of NO<sub>x</sub> are positively correlated with area source emissions and both point and area source emissions affect ozone production. The linear relationship and strong correlation suggests that reductions of NO<sub>x</sub> emissions (from both point and area sources) should reduce ozone levels. Appendix G-8 shows that CMAQ generally underestimates ozone aloft, and because ozone, as shown in this analysis, is positively correlated with NO<sub>x</sub> point source emissions, CMAQ may not adequately demonstrate or capture the efficacy of NO<sub>x</sub> point source emissions controls, and may underestimate the role of transported ozone in Maryland.

## **Future Work**

This study has laid the groundwork for a more rigorous study relating both point and area sources (on, for example, the county scale) of NO<sub>x</sub> to vertical ozone profiles. Because EPA regulates surface ozone, an additional examination should focus on the relationship between surface ozone and the integrated NO<sub>x</sub> emissions (from point and area sources) encountered over a two day period. This study examined data from 1997-2003. In 2003, large scale reductions of point source NO<sub>x</sub> emissions were implemented. It would be enlightening to determine how these reductions impacted vertical profiles and surface measurements of ozone in years subsequent to the NO<sub>x</sub> SIP Call.

## References

Colarco, P.R., M.R. Schoeberl, B.G. Doddridge, L.T. Marufu, O. Torres, and E.J. Welton, 2004. Transport of smoke from Canadian forest fires to the surface near Washington, D.C.: Injection height, entrainment, and optical properties, *Journal of Geophysical Research*, 109, D06203.

Taubman, B.F., Hains, J.C., Thompson, A.M., Marufu, L.T., Doddridge, B.G., Stehr, J.W., Piety, C.A., Dickerson, R.R., 2006. Aircraft vertical profiles of trace gas and aerosol pollution over the mid-Atlantic United States: Statistics and meteorological cluster analysis, *Journal of Geophysical Research*, **111**, D10S07.

Hains, J.C., Taubman, B.F., Thompson, A.M., Marufu, L.T., Doddridge, B.G., Stehr, J.W., Dickerson, R.R., 2007. A clustering methodology to identify distinct chemical events in the troposphere using aircraft trace gas and aerosol vertical profiles, manuscript in preparation.